J Neurophysiol 97: 283–295, 2007.
First published October 18, 2006; doi:10.1152/jn.00634.2006.

Pre- and Postsynaptic Activation of M-Channels By a Novel Opener Dampens Neuronal Firing and Transmitter Release

Asher Peretz,[1] Anton Sheinin,[1] Cuiyong Yue,[3] Nurit Degani-Katzav,[1] Gilad Gibor,[1] Rachel Nachman,[1] Anna Gopin,[2] Eyal Tam,[1] Doron Shabat,[2] Yoel Yaari,[3] and Bernard Attali[1]

[1]*Department of Physiology and Pharmacology, Sackler Faculty of Medicine,* [2]*School of Chemistry, Faculty of Exact Sciences of Tel-Aviv University, Tel Aviv; and* [3]*Department of Physiology, Hebrew University–Hadassah Faculty of Medicine, Jerusalem, Israel*

Submitted 17 June 2006; accepted in final form 16 October 2006

Peretz A, Sheinin A, Yue C, Degani-Katzav N, Gibor G, Nachman R, Gopin A, Tam E, Shabat D, Yaari Y, Attali B. Pre- and postsynaptic activation of M-channels by a novel opener dampens neuronal firing and transmitter release. *J Neurophysiol* 97: 283–295, 2007. First published October 18, 2006; doi:10.1152/jn.00634.2006. The M-type K^+ current (M-current), encoded by Kv7.2/3 (KCNQ2/3) K^+ channels, plays a critical role in regulating neuronal excitability because it counteracts subthreshold depolarizations. Here we have characterized the functions of pre- and postsynaptic M-channels using a novel Kv7.2/3 channel opener, NH6, which we synthesized as a new derivative of *N*-phenylanthranilic acid. NH6 exhibits a good selectivity as it does not affect Kv7.1 and I_{KS} K^+ currents as well as NR1/NR2B, AMPA, and $GABA_A$ receptor-mediated currents. Superfusion of NH6 increased recombinant Kv7.2/3 current amplitude (EC_{50} = 18 μM) by causing a hyperpolarizing shift of the voltage activation curve and by markedly slowing the deactivation kinetics. Activation of native M-currents by NH6 robustly reduced the number of evoked and spontaneous action potentials in cultured cortical, hippocampal and dorsal root ganglion neurons. In hippocampal slices, NH6 decreased somatically evoked spike afterdepolarization of CA1 pyramidal neurons and induced regular firing in bursting neurons. Activation of M-channels by NH6, potently reduced the frequency of spontaneous excitatory and inhibitory postsynaptic currents. Activation of M-channels also decreased the frequency of miniature excitatory (mEPSC) and inhibitory (mIPSC) postsynaptic currents without affecting their amplitude and waveform, thus suggesting that M-channels presynaptically inhibit glutamate and GABA release. Our results suggest a role of presynaptic M-channels in the release of glutamate and GABA. They also indicate that M-channels act pre- and postsynaptically to dampen neuronal excitability.

INTRODUCTION

The M-channels generate a subthreshold, noninactivating voltage-gated K^+ current (M-current) that plays an important role in controlling excitability of many types of neurons (Brown and Yu 2000; Brown 1988; Jentsch 2000; Rogawski 2000). M-channels are thought to mediate early spike frequency adaptation by generating a medium afterhyperpolarization (mAHP) (Brown and Adams 1980; Gu et al. 2005; Peters et al. 2005; Storm 1990). Recently, it was also found that M-current activates during the spike afterdepolarization (ADP), limiting its amplitude and duration and thus preventing the conversion of a single spike to a high-frequency burst of spikes (Yue and Yaari 2004).

The heterotetramer channel complex Kv7.2/3 belonging to the Kv7 (KCNQ) family of voltage-gated K^+ channels was identified as the molecular correlate of the native M-current (Shah et al. 2002; Wang et al. 1998). Kv7.4 and Kv7.5 subunits can also co-assemble with Kv7.3 to produce K^+ currents the properties of which are similar to those of the M-current (Lerche et al. 2000; Schroeder et al. 2000). Reflecting their physiological importance, mutations of the Kv7.2 and Kv7.3 genes have been identified as causes of myokymia and of benign familial neonatal convulsions, a neonatal form of epilepsy (Biervert et al. 1998; Dedek et al. 2001; Singh et al. 1998). Interestingly, M-channels were recently found to be expressed in regions of the nervous system involved in neuropathic pain, such as dorsal and ventral horn of the spinal cord, as well as sensory neurons (Cooper and Jan 2003; Passmore et al. 2003). Immunocytochemical studies have shown a widespread pre- and postsynaptic localization of Kv7.2 and Kv7.3 subunits (Cooper and Jan 2003; Cooper et al. 2000, 2001; Geiger et al. 2006; Weber et al. 2006). A prominent axonal localization at the nodes and initial segments was also recently found (Chung et al. 2006; Devaux et al. 2004; Pan et al. 2006).

Pharmacological targeting of M-channels is of great clinical interest. Blockers (e.g., linopirdine and XE991) (Aiken and Brown 2000; Schnee and Brown 1998; Wang et al. 1998) are potentially useful as cognitive enhancers and as drug templates for the treatment of Alzheimer's disease, whereas openers (e.g., retigabine) (Rundfeldt and Netzer 2000; Tatulian et al. 2001; Wickenden et al. 2000) are actively evaluated for the treatment of neuronal hyperexcitability like migraine, epilepsy, and neuropathic pain (Cooper and Jan 2003; Robbins 2001). Importantly, the design of new modulators of M-currents provides valuable pharmacological tools to study the physiological roles of these currents in the normal and diseased nervous system.

Recently, we showed that meclofenamic acid and diclofenac, two derivatives of *N*-phenylanthranilic acid and currently used as nonsteroidal antiinflammatory drugs (NSAIDs), act as novel Kv7.2/3 channel openers (Peretz et al. 2005). Here we have synthesized a novel molecule, NH6, using diclofenac as a primary template, to characterize the functions of pre- and postsynaptic M-channels. Our data indicate that the NH6 compound is an opener of M-channels by causing a hyperpolarizing shift of the voltage activation curve and by slowing the deactivation kinetics. M-channel activation by NH6 efficiently depresses neuronal excitability by presynaptic and postsynaptic mechanisms.

Address for reprint requests and other correspondence: B. Attali, Dept. of Physiology and Pharmacology, Sackler Faculty of Medicine, Tel Aviv University, Tel Aviv 69978, Israel (E-mail: battali@post.tau.ac.il).

The costs of publication of this article were defrayed in part by the payment of page charges. The article must therefore be hereby marked "*advertisement*" in accordance with 18 U.S.C. Section 1734 solely to indicate this fact.

METHODS

All animal experiments were approved by the animal research ethics committees of Tel Aviv and Hebrew Universities and were in accordance with the "Guide for the Care and Use of Laboratory Animals" (1996; National Academy of Sciences, Washington DC).

Synthesis of compound NH6

The detailed procedures for synthesis and chemical analysis of compound NH6 will be described elsewhere. Briefly, the carboxylic acid of diclofenac (50 mg, 0.17 mmol) was dissolved in dry dichloromethane (DCM). Catalytic amounts of 4-dimethyl aminopyridine and diethylene glycol (0.08 ml, 0.85mmol) were added. The stirred mixture was cooled to 0°C, and dicyclohehyl carbodiimide (52.6 mg, 0.255 mmol) dissolved in DCM was added dropwise. The suspension was then stirred at 0°C for 30 min and monitored by thin layer chromatography (EtOAc:He = 1:1). The solid was removed by filtration and washed with DCM. The filtrate was concentrated under reduced pressure and chromatographed over silica gel to afford the pure ester NH6. ^{1}HNMR (200 MHz, $CDCl_3$): δ = 7.35 ppm (2H, d, J = 8); 7.19–7.06 (2H, m); 6.99 (1H, d, J = 8); 6.96 (1H, d, J = 8.); 6.56 (1H, d, J = 8); 4.35 (2H, m); 3.8 (2H, s); 3.65–3.75 (4H, m); 3.53–3.57 (2H, m). MS (FAB): [$C_{18}H_{19}C_{l2}NO_4$] 383.0.

Cell line culture and transfection

Chinese hamster ovary (CHO) cells were grown in Dulbecco's modified Eagle's medium supplemented with 2 mM glutamine, 10% fetal calf serum and antibiotics. Briefly, 40,000 cells seeded on poly-D-lysine-coated glass coverslips (13 mm diam) in a 24-multiwell plate were transfected with pIRES-CD8 (0.5 μg) as a marker for transfection, and with Kv7.2 (0.5 μg) and Kv7.3 (0.5 μg). For electrophysiology, transfected cells were visualized ~40 h after transfection, using the anti-CD8 antibody-coated beads method (Jurman et al. 1994). Transfection was performed using Fugene 6 (Roche, Indianapolis IN) according to the manufacturer's protocol.

Dorsal root ganglion neuron cultures

Dorsal root ganglion (DRG) neurons were dissected from 2- to 4-day-old ICR mice killed by decapitation. DRGs were placed in Hank's balanced saline solution (HBSS) and prepared by enzymatic dissociation. Briefly, after a 30-min incubation in 5 mg/ml dispase, 2 mg/ml collagenase type 1A, and 0.1 mg/ml DNase (Invitrogen/Gibco, Carlsbad, CA) in Ca^{2+} and Mg^{2+}-free HBSS, the ganglia were mechanically triturated with a fire-polished glass Pasteur pipette. The ganglia were then centrifuged for 5 min at 80 *g* and resuspended in DMEM supplemented with 2 mM L-glutamine, 16.5 mM $NaCO_3$, 6 g/l glucose, 5 ml penicillin/streptomycin, and 10% fetal calf serum. For electrophysiological recording, dissociated neurons were plated on 13-mm glass coverslips, previously coated with poly-D-lysine (1 mg/ml) and laminin (10 μg/ml) and used at 2–6 days in culture.

Cortical and hippocampal neuron cultures

Sprague Dawley rat embryos (E18) were removed by caesarian section, and their cortices and hippocampi were dissected out. The tissue was digested with papain for 20 min, triturated to a single-cell suspension, and plated at a density of 40,000 cells/ml on a substrate of bovine collagen type IV and 100 μg/ml poly-L-lysine in 13-mm-diam glass coverslips of a 24-multiwell plate. The culture medium consisted of modified Eagle's medium containing 5% horse serum (Biological Industries, Beit HaEmek, Israel), B-27 neuronal supplement (Invitrogen), 100 U/ml penicillin, 100 μg/ml streptomycin, and 2 mM glutamine. D-glucose was supplemented to a final concentration of 6 g/l. Cytosine-1-D-arabinofuranoside (5 μM) was added after 5 days to arrest glial cell proliferation. For electrophysiological recordings, cortical and hippocampal neurons were used at 10–15 days in culture. All cultures were maintained at 37°C in humidified air containing 5% CO_2.

Hippocampal slices

Transverse hippocampal slices were prepared from adult Sabra rats (150–200 g). Animals were anesthetized with ether or isoflurane (3–4%) and decapitated with a guillotine. The brain was removed and immediately immersed in ice-cold oxygenated (95% O_2-5% CO_2) dissection saline solution. The caudal two-thirds of one hemisphere (containing 1 hippocampus) were glued to the stage of a Vibratome (Leica). Transverse slices (400 μm thick) were cut from the region of the hemisphere containing the anterior hippocampus, and the hippocampal portion was dissected out. The slices were transferred to an incubation chamber containing oxygenated saline solution at room temperature (21–24°C), where they were allowed to recover for ≥1 h. The slices were transferred one at a time to an interface slice chamber and perfused from below with oxygenated (95% O_2-5% CO_2) saline solution at 33.5°C. The upper surface of the slices was exposed to the humidified gas mixture. The standard saline solution contained (in mM): 124 NaCl, 3.5 KCl, 2 $MgSO_4$, 1.6 $CaCl_2$, 26 $NaHCO_3$, and 10 D-glucose (pH 7.3). To obtain Ca^{2+}-free saline solution, the $CaCl_2$ was replaced with equimolar $MgCl_2$. The saline solutions contained also the glutamate receptor antagonists 6-cyano-7-nitro-quinoxaline-2,3-dione (CNQX; 15 μM) and 2-amino-5-phosphono-valeric acid (APV; 50 μM) to block fast excitatory postsynaptic potentials (EPSPs), and the $GABA_A$ receptor antagonist picrotoxin (100 μM) to block fast inhibitory postsynaptic potentials (IPSPs). Other drugs were added to the saline solution as indicated.

Electrophysiology

Voltage-clamp recordings in CHO cells were performed 40 h after transfection, using the whole cell configuration of the patch-clamp technique (Hamill et al. 1981). Signals were amplified using an Axopatch 200B patch-clamp amplifier (Molecular Devices, Sunnyvale, CA), sampled at 2 kHz and filtered at 800 Hz via a 4-pole Bessel low-pass filter. Data were acquired using pClamp 8.1 software (Molecular Devices) and an Elonex Pentium III computer in conjunction with a DigiData 1322A interface (Molecular Devices). The patch pipettes were pulled from borosilicate glass (Warner Instrument) with a resistance of 2–5 MΩ. For K^+ current recordings in CHO cells, the intracellular pipette solution contained (in mM) 130 KCl, 1 $MgCl_2$, 5 K_2ATP, 5 EGTA, and 10 HEPES, adjusted with KOH to pH 7.4 (290 mosM). The saline solution contained (in mM) 140 NaCl, 4 KCl, 1.8 $CaCl_2$, 1.2 $MgCl_2$, 11 glucose, and 5.5 HEPES, adjusted with NaOH to pH 7.4 (310 mosM). Series resistances (3–13 MΩ) were compensated (75–90%) and periodically monitored. The impact of NH6 on NR1/NR2B receptor currents was checked in transfected CHO cells. In these experiments, the saline solution contained 10 μM glutamate with and without 1 mM L-alanine. The pipette solution was similar to the in the preceding text except that KCl was replaced with CsCl.

Current-clamp recordings in primary cultured neurons were performed 10–14 days after neuron plating. The patch pipettes were filled with (in mM) 135 KCl, 1 K_2ATP, 1 MgATP, 2 EGTA, 1.1 $CaCl_2$, 5 glucose, and 10 HEPES, adjusted with KOH at pH 7.4 (315 mosM). The saline solution contained (in mM) 140 NaCl, 4 KCl, 2 $CaCl_2$, 2 $MgCl_2$, 5 glucose, and 0 HEPES, adjusted with NaOH at pH 7.4 (325 mosM). A liquid junction potential of about −15.6 mV was measured between the intracellular and saline solutions and corrected on-line. For evoking action potentials, 50- to 300-pA square current pulses were injected into the cells for 800 ms. Recordings were sampled at 5 kHz and filtered at 2 kHz via a 4-pole Bessel low-pass filter. For voltage-clamp measurements in cultured neurons, the patch pipettes were filled with (in mM) 90 K-acetate, 40 KCl, 3 $MgCl_2$, 2 K_2ATP, and 20 HEPES, adjusted with KOH at pH 7.4 (310–315 mosM). The

saline solution contained (in mM) 120 NaCl, 23 $NaHCO_3$, 3 KCl, 2.5 $CaCl_2$, 1.2 $MgCl_2$, 11 glucose, and 0.5 HEPES, adjusted with NaOH at pH 7.4 (325 mosM), and supplemented with 0.5 μM tetrodotoxin (TTX). For recording excitatory postsynaptic currents (EPSCs), the saline solution contained (in mM) 160 NaCl, 2.5 KCl, 10 HEPES, 10 glucose, and 2 $CaCl_2$; pH 7.3 (325 mosM), to which 10 μM picrotoxin and 10 μM bicuculline methyl iodide were added. The intracellular solution consisted of 130 K-gluconate, 10 KCl, 5 EGTA, 10 HEPES, 1 $MgCl_2$, 2 Na ATP, 0.5 $CaCl_2$; pH 7.2 (310–315 mosM). For isolating miniature EPSCs (mEPSCs), 0.5 μM TTX was added to the latter saline solution, while the intracellular solution was composed of (in mM) 125 $CsMeSO_3$, 15 CsCl, 10 HEPES, 0.5 $CaCl_2$, 3 $MgCl_2$, 5 Cs_4 BAPTA, and 2 Na ATP. For isolating miniature IPSCs (mIPSCs), the saline solution was the same as above, but containing also 10 μM 1,2,3,4-tetrahydro-6-nitro-2,3-dioxo-benzo[f]quinoxaline-7-sulfonamide (NBQX), 200 μM D-APV, and 0.5 μM TTX; the intracellular solution consisted of (in mM) 144 CsCl, 10 HEPES, 1.1 EGTA, 0.1 $CaCl_2$, 5 $MgCl_2$, Na ATP 2, pH 7.2. Acquisition of EPSCs, mEPSCs, and mIPSCs data was performed with Synapse (Synergistic Systems, Silver Spring, MD), a Macintosh-based electrophysiological software package. Peak detection and further analysis were performed with Igor Pro 4.0 (Wavemetrics, Lake Oswego, OR) and custom-written macros.

Current-clamp recordings from the somata of CA1 pyramidal cells were made using sharp, K-acetate-filled (4 M) glass microelectrodes (70–100 MΩ). An active bridge circuit in the amplifier (Axoclamp 2A; Molecular Devices) allowed simultaneous injection of current and measurement of membrane potential. The bridge balance was carefully monitored and adjusted before each measurement. The pyramidal cells accepted for this study had stable resting potentials of at least −60 mV and overshooting action potentials.

Voltage-clamp measurements in *Xenopus* oocytes were performed as previously described (Peretz et al. 2005). The cDNAs encoding the various Kv channels including Kv1.2, Kv1.5, Kv2.1, Kv7.1/KCNE1, Kv7.1, and Kv7.2/3 were linearized and the corresponding cRNAs were synthesized using the T7 or SP6 RNA polymerases. Briefly, two-electrode voltage-clamp measurements were performed 3–5 days after cRNA microinjection into oocytes. Oocytes were bathed in a modified ND96 saline solution containing (in mM) 96 NaCl, 2 KCl, 1 $MgCl_2$, 0.1 $CaCl_2$, and 5 HEPES, titrated to pH 7.4 with NaOH. Whole cell currents were recorded at room temperature (20–22°C) using a GeneClamp 500 amplifier (Molecular Devices). Glass microelectrodes (A-M Systems) were filled with 3 M KCl and had tip resistances of 0.2–0.5 MΩ. Stimulation of the preparation, data acquisition and analyses were performed using the pClamp 6.02 software and a 586 personal computer interfaced with a Digidata 1200 interface. Current signals were filtered at 0.5 kHz and digitized at 2 kHz.

Chemicals and drugs

Except when indicated, all drugs were purchased from Sigma (St Louis, MO). Bicuculline, NBQX, CNQX, and APV were purchased from Tocris (Bristol, UK). TTX was purchased from Alomone Labs (Jerusalem, Israel). Retigabine was kindly provided by Dr. H. Lerche (Ulm University).

Data analyses

Data analysis was performed using the Clampfit program (pClamp 8.1), Microsoft Excel (Microsoft), SigmaPlot 8.0 and Prism 4.0 (GraphPad). Leak subtraction was performed off-line, using the Clampfit program of the pClamp 8.1 software. To analyze the Kv7.2/3 channel deactivation, a single-exponential fit was applied to the tail currents. Chord conductance (G) was calculated by using the following equation

$$G = I/(V - V_{rev})$$

where I corresponds to the current amplitude measured at the end of the pulse and V_{rev} is the calculated reversal potential (−90 mV in CHO cells and –98 mV in *Xenopus* oocytes). G was estimated at various test voltages and normalized to the maximal conductance value, G_{max}. Activation curves were fitted by one Boltzmann equation

$$G/G_{max} = 1/\{1 + \exp[(V_{50} - V)/s]\}$$

where V_{50} is the voltage at which the conductance is half-activated and s is the slope factor.

All data were expressed as means ± SE. Statistically significant differences were assessed by Student's t-test with a significance level of $P < 0.05$. Analysis of mEPSCs and mIPSCs included evaluation of the individual events, as well as the average event amplitude, 10–90% rise time and decay time constant. Statistical evaluation of the drug-induced effect on the cumulative probability of amplitude, decay time constant and frequency (interevent intervals) was performed with the Kolmogorov-Smirnov nonparametric two-sample test with a significance level of $P = 0.001$.

Immunocytochemistry

Cortical neurons were grown in culture for 10–14 days on 13-mm-diam coated glass coverslips in 24-well plates. Cells were carefully rinsed for 10 min in phosphate-buffered saline (PBS), and the neurons subsequently were fixed for 20 min in 4% paraformaldehyde in PBS. After extensive washes in PBS, the cells were permeabilized by incubation with 10% normal goat serum (NGS) in PBS containing 0.2% Triton X-100. Cells were then washed for 10 min in PBS containing 1% NGS. Neurons were incubated at 4°C overnight with anti-Kv7.2 and anti-Kv7.3 channel antibodies diluted in PBS containing 1% NGS. A rabbit polyclonal antibody to Kv7.2 (1:500; Alomone Labs) was combined with a goat polyclonal antibody to Kv7.3 (N19: 1:50; Santa Cruz Biotechnology, Santa Cruz, CA); alternatively a rabbit polyclonal antibody to Kv7.3 (1:100; Alomone Labs) was combined with a goat polyclonal antibody to Kv7.2 (N19:1:50; Santa Cruz Biotechnology). After a wash in PBS, cells were incubated for 1 h at room temperature with secondary antibodies, CY2-conjugated anti-rabbit IgG (1:200; Jackson Immunoresearch) and RRX-conjugated anti-goat IgG (1:100; Jackson Immunoresearch). Neurons were viewed and digital images taken using a Leica SP2 confocal microscope.

RESULTS

NH6 acts as an opener of Kv7.2/3 K^+ channels

We have recently showed that two NSAID drugs derivatives of *N*-phenylanthranilic acid, diclofenac and meclofenamic acid, act as novel openers of Kv7.2/3 channels (Peretz et al. 2005). The potent opener activity of these two fenamate compounds toward Kv7.2/3 channels led us to design the synthesis of a new molecule, NH6, a derivative of diclofenac. For this purpose, we added a diethylene glycol tail to the carboxylic acid functionality of the molecule (Fig. 1*A*). As shown in Fig. 1*B*, NH6 was a potent opener of recombinant Kv7.2/3 channels heterologously expressed in CHO cells. In a train protocol, when membrane potential was stepped every 30 s from −90 to −50 mV, and once current amplitude stabilized, external application of 25 μM NH6 rapidly produced an ≤4.2-fold increase in current amplitude ($n = 10$; Fig. 1, *C* and *D*). The onset of the drug action was fast because within 1 min of superfusion, NH6 significantly raised the

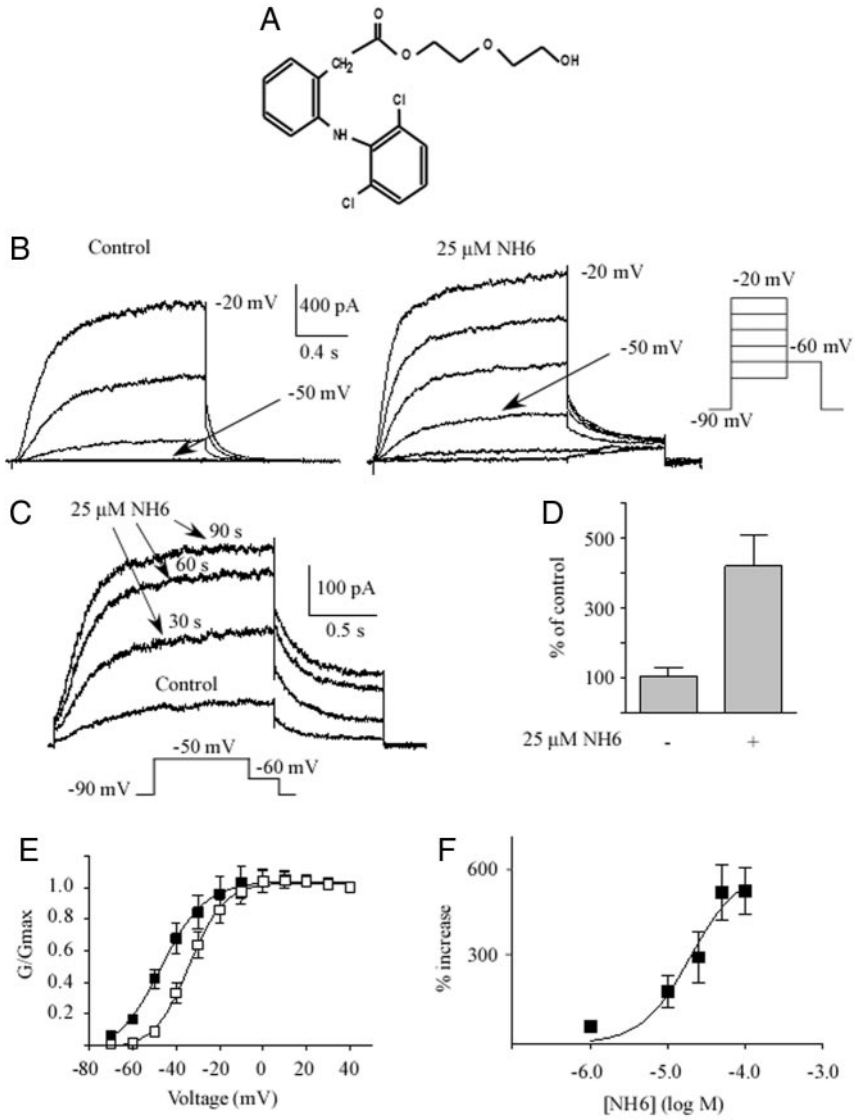

FIG. 1. Opener properties of NH6 on Kv7.2/3 currents expressed in Chinese hamster ovary (CHO) cells. *A*: chemical structure of NH6. *B*: representative traces recorded from the same cell before (*left,* control) and after (*right*) external application 25 μM NH6. The membrane potential was stepped from −90 mV (holding potential) to −20 mV for 1.5-s pulse duration in 10-mV increments, followed by a 0.75-s step to −60 mV. *C*: current traces were recorded from the same cell in the absence (control) and presence of 25 μM NH6. In this train protocol, the cells were stepped from −90 to −50 mV every 30 s for 1.5-s pulse duration. *D*: percentage of the current recorded at −50 mV is shown in the presence (+) or absence (−) of 25 μM NH6, the latter being the control of 100% (n = 10). *E*: normalized conductance (G/G_{max}) was plotted as a function of the test voltages, for control (□) and 25 μM NH6-treated cells (■). The activation curves were fitted using 1 Boltzmann function (n = 7). *F*: dose-response curve of NH6 opener activity for Kv7.2/3 channels. The potency of NH6 was determined by the percentage of current enhancement at −50 mV, plotted as a function of NH6 concentration and fitted by a sigmoidal function yielding an EC_{50} value of 18 ± 4 μM (n = 7).

current (Fig. 1*C*). The opener action was time dependent and reached its maximum steady-state value after about 2 min of drug exposure. The effects of NH6 appear to be voltage dependent. As the test potentials were more positive and approached the saturating values of the activation curve (above −30 mV), the effects of NH6 on Kv7.2/3 current amplitude became weaker. Figure 1*B* describes the NH6-induced enhancement of Kv7.2/3 current at physiologically relevant voltages (from −70 to −20 mV; holding potential: −90 mV). It is clear that the current enhancement produced at −50 mV was much larger than that evoked at −20 mV. When these data were expressed as conductance/voltage relationships (Fig. 1*E*), it became evident that the NH6 effect is due to a leftward shift of about −18.7 mV in the Kv7.2/3 activation curve (from V_{50} = −29.9 ± 2.8 mV to V_{50} = −48.6 ± 0.5 mV; n = 7; $P <$ 0.01) without a change in slope (s = 8.3 ± 1.6 mV and s = 11.6 ± 3.1 mV without and with 25 μM NH6, respectively; n = 7). As is evident from comparing tail currents (Fig. 1*B*), NH6 also slowed down the deactivation kinetics of Kv7.2/3 channels (τ_{deact} = 82 ± 7 ms and τ_{deact} = 132 ± 8 ms before and after NH6 exposure, respectively, at −60-mV tail potential; n = 6; $P <$ 0.02). The action of NH6 was concentration dependent. When tested with command pulses to −50 mV, this dependence yielded an EC_{50} value of 18 ± 4 μM (Fig. 1*F*; n = 7). Similar results were obtained in *Xenopus* oocytes with an NH6-induced enhancement of Kv7.2/3 current of about twofold at −40 mV (Table 1).

Selectivity of NH6 toward other ion channels

To characterize the selectivity of NH6, we examined at relevant membrane potentials its action on other voltage-gated K^+ channels (Kv) expressed in *Xenopus* oocytes. The results, summarized in Table 1, indicate that NH6 (25 μM) did not affect Kv1.2, Kv1.5 and Kv2.1, homomeric Kv7.1 and heteromeric Kv7.1/KCNE1 currents. Likewise, NH6 (5–25 μM) had no effect on recombinant NR1/NR2B *N*-methyl-D-aspartate (NMDA) receptor channels in transfected CHO cells. Finally, we tested the impact of 25 μM NH6 on native postsynaptic AMPA and $GABA_A$ currents by measuring the amplitude of mEPSCs and mIPSCs, respectively, in cultured hippocampal neurons (Table 1, see also Figs. 7 and 9). NH6 did not affect mEPSCs and mIPSCs amplitudes.

TABLE 1. *Specificity of NH6 effects on other ion channel subtypes*

Ion Channel Type	Percent of Control Current Amplitude
Kv1.2 (−20 mV)	98 ± 9
Kv1.5 (0 mV)	95 ± 8
Kv2.1 (0 mV)	105 ± 9
Kv7.1 (−40 mV)	96 ± 6
Kv7.1/KCNE1 [I_{ks}] (0 mV)	102 ± 15
Kv7.2/3 (−40 mV)	195 ± 16*
NR1/NR2B	110 ± 5
Hippocampal AMPA currents	95 ± 6
Hippocampal $GABA_A$ currents	93 ± 4

The specificity of NH6 (25 μM) toward Kv channels was tested in *Xenopus* oocytes by measuring from a −80-mV holding potential, the current amplitude of various Kv channels including Kv1.2 (at −20 mV), Kv1.5, Kv2.1, and Kv7.1/KCNE1 (at 0 mV) and Kv7.1 and Kv7.2/3 (at −40 mV). The effect of NH6 on recombinant NR1/NR2B *N*-methyl-*d*-aspartate receptor channels was measured in transfected Chinese hamster ovary cells and that on native AMPA and $GABA_A$ receptor-mediated currents was, respectively, recorded from miniatues excitatory and inhibitory post synaptic currents in cultured hippocampal neurons as described in METHODS. The effects of NH6 were expressed as percentage of the control amplitude, measured under the same conditions in the absence of the drug. Data are expressed as means ± SE of 5–8 separate experiments. *$P < 0.01$.

NH6 is an opener of M-channels in hippocampal and neocortical neurons

To explore whether NH6 is also an opener of native M-channels, we first examined its effects in rat hippocampal and neocortical pyramidal-like neurons grown in culture for 10–14 days. Figure 2*A* shows by means of double immunofluorescence staining that Kv7.2 and Kv7.3 subunits are co-localized in rat primary hippocampal neurons. The polyclonal antibodies which we used were specific and recognized selectively KCNQ2 and KCNQ3 channel proteins when expressed in CHO cells (Fig. 2*A*). The staining for both Kv7.2 and Kv7.3 is most prominent in the somata and is also present along the neuronal processes. No significant immunofluorescence was observed when the antibodies were preadsorbed with their respective antigenic peptide (Fig. 2*A*). Similar results were obtained in cultured neocortical neurons (Peretz et al. 2005; data not shown).

For voltage-clamp rcordings, neurons were held at −90 mV. The voltage protocol used to isolate M-currents was first to step to −20 mV for 8 s and then to step back to −50 mV (Shah et al. 2002; Tatulian et al. 2001). This protocol disclosed a tiny, slowly deactivating K^+ current corresponding to M-current in both hippocampal and neocortical neurons (Fig. 2, *B–D*). This current was nearly completely blocked by 10 μM linopirdine (Fig. 2*B*), a blocker of Kv7.2/3 channels (Wang et al. 1998). The M-current amplitude was isolated by subtracting the currents evoked before and after 10 μM linopirdine application (Fig. 2*B*, *bottom*). To determine the activating effect of NH6, the M-current was first recorded in the absence of the opener by measuring the extent of the linopirdine-sensitive current (Fig. 2*C*, subtracted control black trace); this current amplitude was considered as the 100% of control M-current. Then after washout of linopirdine, the same neuron was superfused with

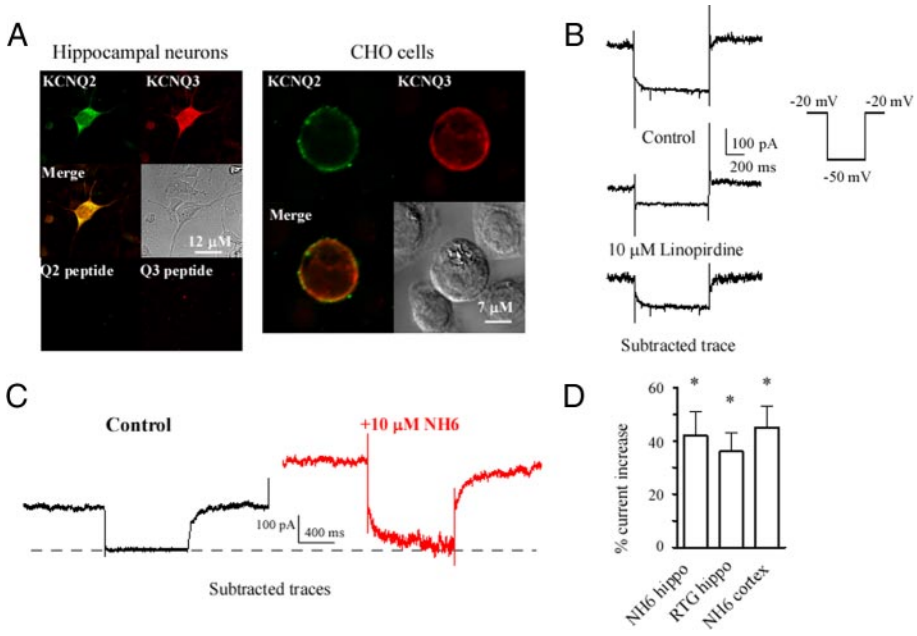

FIG. 2. NH6 enhances the M-current in rat cortical and hippocampal neurons. *A*: double immunofluorescence staining showing that Kv7.2 and Kv7.3 subunits are co-localized in rat primary hippocampal neurons (*left*). Specific immuno-detection of KCNQ2 and KCNQ3 α subunits in CHO cells co-transfected with KCNQ2 and KCNQ3 cDNAs (*right*). No significant immunofluorescence was observed when the antibodies were preadsorbed with their respective antigenic peptide (*bottom left*). *B*: representative record from a cortical neuron held at −90 mV. To isolate M-currents, the membrane potential was first stepped to −20 mV for 8 s and then stepped back to −50 mV. This tiny current was almost completely blocked by 10 μM linopirdine. Thus the M-current amplitude could be quantified from the traces obtained by subtracting the currents evoked before and after linopirdine application. *C*: representative subtracted traces of linopirdine-sensitive currents from a hippocampal neuron in the absence (control, black trace) or presence of 10 μM NH6 (red trace). The dotted line indicates the zero current. To check the activating effect of NH6, the M-current was 1st recorded in the absence of the opener by measuring the linopirdine-sensitive current; this current amplitude was considered as the 100% of control M-current. Then after washout of linopirdine, the same neuron was superfused with 10 μM NH6 alone and subsequently with 10 μM NH6 + 10 μM linopirdine, which yields the linopirdine-sensitive current in the presence of the opener. *D*: percentage of the current increase above control by the presence of 10 μM NH6 in hippocampal ($n = 5$, $P < 0.01$) and cortical neurons ($n = 5$, $P < 0.01$) and by retigabine (RTG) in hippocampal neurons ($n = 5$, $P < 0.01$).

10 μM NH6 alone and subsequently with 10 μM NH6 + 10 μM linopirdine, which yielded the linopirdine-sensitive current in the presence of the opener (Fig. 2*C*, subtracted NH6 red trace). The difference of the linopirdine-sensitive current without and with the opener provides a measure of the M-current activation and the enhancing effect was expressed as the percentage of current increase above the 100% control M-current (Fig. 2*D*). As illustrated in Fig. 2, *C* and *D*, 10 μM NH6 enhanced the M-current in hippocampal neurons by 42 ± 9% (Fig. 2*D*; $n = 5$, $P < 0.01$). Similar results were obtained in cortical neurons, where 10 μM NH6 augmented the M-current by 45 ± 8% (Fig. 2*D*; $n = 7$, $P < 0.01$). By comparison, 10 μM retigabine increased M-current in hippocampal neurons by 36 ± 7% ($n = 5$, $P < 0.01$).

M-channel activation by NH6 inhibits firing of central and peripheral neurons

It is believed that the preponderant role of M-current is to dampen neuronal repetitive discharge. In such a case, NH6, by enhancing this current, should reduce evoked and spontaneous repetitive firing. We first examined this feature in cultured rat neocortical and hippocampal neurons using the current-clamp configuration of the patch-clamp technique. The resting membrane potential of these neurons was close to −60 mV and was maintained at this level by injecting appropriate DC current. Superfusion of 10 μM NH6 reduced by 95 ± 10% and sometimes up to total suppression the number of action potentials evoked by depolarizing current injection in neocortical neurons (800-ms, 50- to 70-pA current pulse; $n = 30$, $P < 0.001$). Figure 3*A* shows a representative experiment in a neocortical neuron. Within ~1 min of external application of NH6, the neuron fired fewer action potentials with a widening of the interspike interval (Fig. 3*A*, *2nd row*). After 2 min of exposure to the drug, only one spike could be evoked by the same depolarizing current (Fig. 3*A*, *3rd row*). Like in transfected CHO cells, the NH6 effects in neurons were time dependent and reached steady state after ~2 min of drug exposure. Within 2 min of washout of the compound, the neuron recovered its initial spiking activity (Fig. 3*A*, *4th and 5th rows*).

In dense cultures, both neocortical and hippocampal neurons displayed spontaneous spiking activity. As illustrated in Fig. 3*B*, superfusion of NH6 in a neocortical neuron dose-dependently produced a profound depression of spontaneous action potentials with 61 ± 8, 80 ± 7, and 96 ± 3% inhibition of spontaneous spiking, respectively, produced by exposure of 5, 10, and 20 μM NH6 ($n = 5$–10, $P < 0.01$). This depression was quickly reversed by drug washout (Fig. 3*B*). Very similar results were obtained in cultured hippocampal neurons (data not shown). In cultured neocortical and hippocampal neurons, NH6 (10 μM) also caused a rapid hyperpolarization (by −7 ± 3 mV; $n = 21$, $P < 0.01$).

Recently, it was found that Kv7.2 and Kv7.3 subunits are expressed in sensory DRG neurons involved in nociceptive signaling pathways (Passmore et al. 2003). There is strong evidence that hyperexcitability and ectopic discharge, which underlie allodynia, hyperalgesia, and ongoing pain, are mediated by abnormal activity of a variety of ion channels (Birch et al. 2004). Therefore we examined in the current-clamp configuration whether NH6 affects spike activity of cultured mouse DRG neurons (Fig. 3*C*). Spike trains were evoked by depolarizing current pulses (70–100 pA, 400 ms). The spikes were associated with very large afterhyperpolarizations (AHPs). External application of 15 μM NH6 potently and reversibly blocked the evoked spikes with 82 ± 7% inhibition ($n = 6$, $P < 0.01$; Fig. 3*C*). NH6 significantly hyperpolarized the DRG membrane potential by −8 ± 3 mV ($n = 6$, $P < 0.05$). Very similar results were obtained with 15 μM retigabine (data not shown).

M-channel activation by NH6 inhibits spike ADP and bursting behavior in hippocampal CA1 pyramidal neurons

Using selective modifiers of M-channels, it was recently shown that these channels critically modulate the firing pattern of hippocampal CA1 pyramidal neurons by limiting the size of the spike ADP (Yue and Yaari 2004). Thus the M-channel

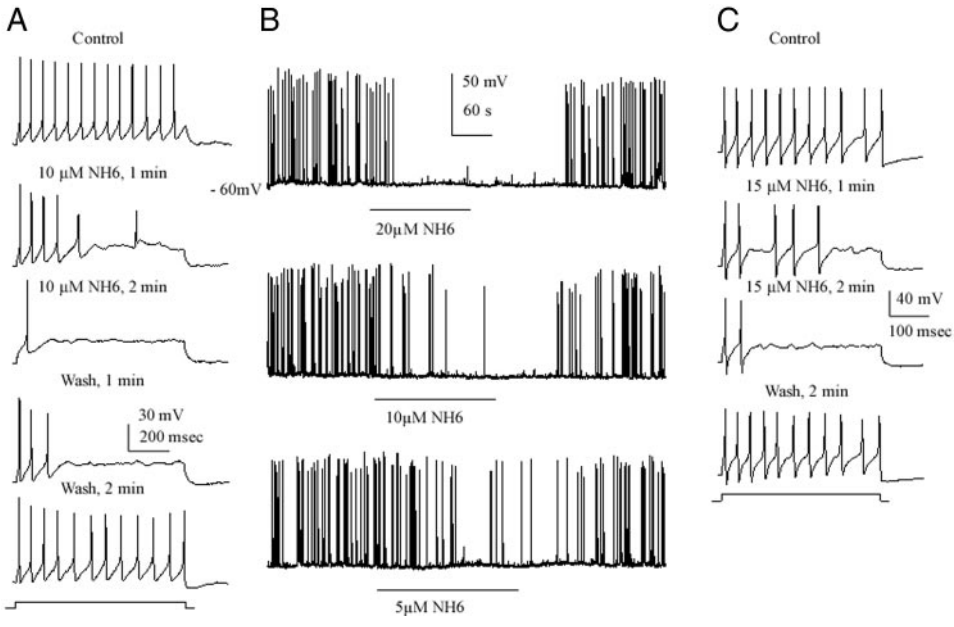

FIG. 3. NH6 inhibits firing of central and peripheral neurons. *A*: rat cortical spiking activity was evoked by a squared depolarizing current pulse (50 pA for 800 ms) before (control), after superfusion with 10 μM NH6, and after drug washout (wash). *B*: rat cortical spontaneous neuronal activity recorded before, during exposure, and wash of NH6 compound (5–20 μM). *C*: mouse DRG neuron spiking activity was evoked by a squared depolarizing current pulse (200 pA for 800 ms) before (control), after superfusion with 15 μM NH6, and after drug washout (wash).

blockers linopirdine and XE991 caused spike ADP facilitation and escalation to burst mode, whereas the M-channel opener retigabine greatly curtailed the spike ADP (Yue and Yaari 2004). Thus we predicted that NH6 would elicit similar effects as those produced by retigabine in CA1 pyramidal cells. In this series of experiments, we used sharp microelectrode recordings in CA1 pyramidal cells in acute hippocampal slices. Effects of M-channel openers on resting membrane potential were counteracted by injecting the neurons with an appropriate DC current to maintain the native resting potential. Unlike retigabine, which decreased the apparent neuron input resistance (Yue and Yaari 2004), NH6 (25 μM) did not significantly modify this parameter (from 36.6 $\pm$ 6.3 to 33.6 $\pm$ 10.9 MΩ; $n = 9$).

In control conditions, injection of long suprathreshold depolarizing current pulses produced accommodating spike trains. In some neurons, as in the one described in Fig. 4*A*, the initial response to high-intensity stimuli was a burst of several spikes (usually 3 or 4; Fig. 4*A, left, top trace*). Superfusion of NH6 (25 μM) caused dispersion of the spike burst (Fig. 4*A, right, top trace*) and in some neurons also decreased the total number of spikes generated by each pulse. Similar results were obtained with retigabine (Fig. 4*B*; $n = 3$). To assess the effects of NH6 on the spike ADP, brief (4 ms) depolarizing current pulses were injected to the neurons to elicit a solitary spike. As shown in Fig. 4*C*, NH6 did not affect spike amplitude but markedly reduced the spike ADP amplitude. In 10 experiments, the decrease in spike ADP by NH6 amounted to ~60% (from 193.8 $\pm$ 49.7 to 117.1 $\pm$ 40.6 mV $\cdot$ ms; $P < 0.05$). Very similar results were obtained with 10 μM retigabine (Fig. 4*D*; $n = 3$) as previously described (Yue and Yaari 2004).

We examined whether activation of M-channels by NH6 would also suppress the low-threshold bursting behavior, which is readily induced in CA1 pyramidal cells by lowering extracellular Ca^2 concentration (Su et al. 2001). As illustrated in Fig. 5*A*, superfusing the slices with nominally Ca^{2+}-free saline solution converted single spiking to burst firing. Adding 25 μM NH6 suppressed bursting while reducing the spike ADP (Fig. 5*A*). These effects of NH6 were similar to those exerted by 10 μM retigabine on low Ca^{2+}-induced bursting (Yue and Yaari 2004) (Fig. 5*B*; $n = 3$).

Activation of M-channels by NH6 reduces the frequency of spontaneous EPSCs in cultured hippocampal neurons

While the depressant effects of NH6 on evoked discharge, the spike ADP and bursting behavior are clearly postsynaptic (somatic) in nature, the inhibition of spontaneous spiking may involve a synaptic site of action. Therefore we have investigated how NH6 modulates synaptic transmission. We first examined the effects of NH6 on spontaneous EPSCs recorded from cultured hippocampal neurons using the voltage-clamp configuration of the patch-clamp technique. Spontaneous EPSCs were recorded at a holding potential of -70 mV and were isolated by pharmacologically blocking $GABA_A$ receptor-mediated inhibitory postsynaptic currents (with 10 μM bicuculline and 10 μM picrotoxin). Under control conditions, EPSC frequency was variable, ranging from 0.4 to 2 Hz and increasing with the density of the hippocampal culture. The main component of spontaneous EPSCs was mediated by AMPA receptors, as EPSCs were mostly blocked by 10 μM NBQX (Fig. 6*A*, *top* and *middle*). A minor fraction of EPSPs resistant to NBQX was abolished by D-2-amino-5-phosphonopentanoic acid (Fig. 6*A*, *bottom*), suggesting that EPSCs are also mediated by NMDA receptors, though to a much lower extent under these experimental recording conditions.

Application of NH6 dose-dependently reduced the frequency of spontaneous EPSCs without significant effect on the amplitude and the kinetics of the currents. Whereas 5 μM NH6 depressed the frequency of EPSCs by 49 $\pm$ 5% of control ($n =$

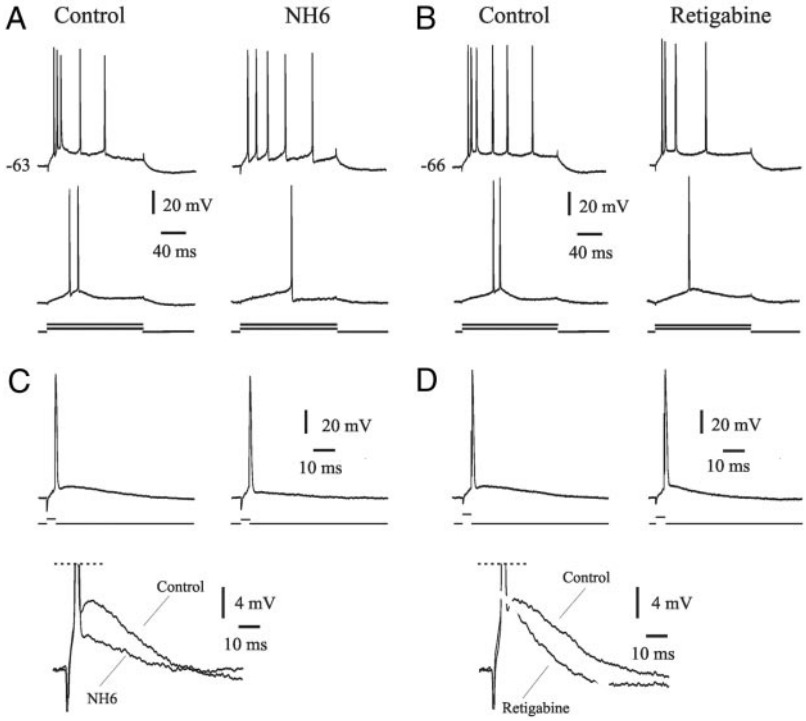

FIG. 4. NH6 and retigabine inhibit CA1 pyramidal neuron intrinsic bursting behavior and reduce the afterdepolarization (ADP) in rat hippocampal slices. *A* and *B*: intracellular recordings of accommodating spike trains evoked by long (200 ms) suprathreshold depolarizing current pulses (700 pA) in the absence (control) and presence of 25 μM NH6 (*A*) and 10 μM retigabine (*B*). *C* and *D*: intracellular recordings of a solitary spike evoked by a brief (4 ms) depolarizing current pulse (1 nA) before (control) and after application of 25 μM NH6 (*C*) and retigabine (*D*). *Insets*: zoom on the ADP as recorded before (control) and after perfusion of NH6 (*C*) and 10 μM retigabine (*D*). In the *bottom panels,* an overlay of the expanded portions of the voltage traces shows the depressing effect of NH6 (*C*) and retigabine (*D*) on ADP.

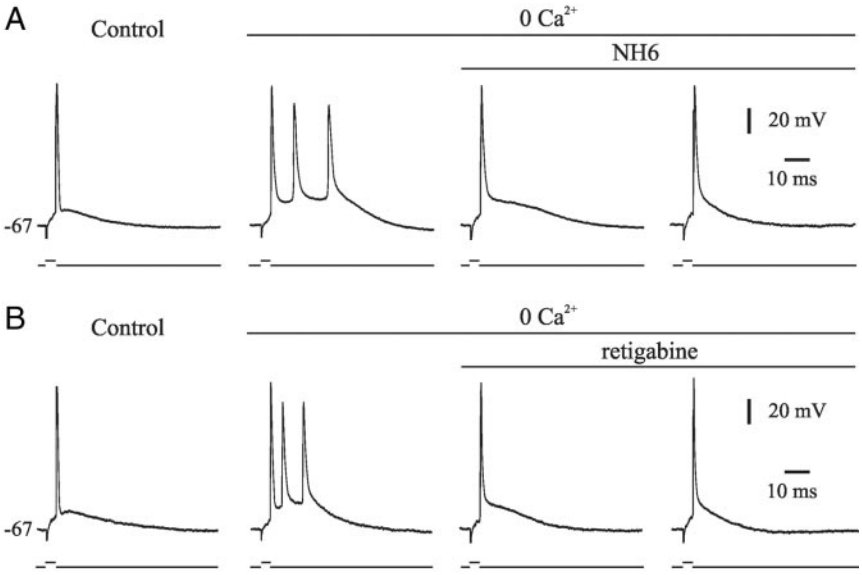

FIG. 5. NH6 and retigabine inhibit intrinsic bursting behavior of CA1 pyramidal neurons evoked by Ca^{2+}-free saline solution in rat hippocampal slices. *A* and *B*: in normal saline solution, CA1 neurons fire a solitary spike in response to a brief depolarizing current stimulus (control). Changing the superfusion medium to a Ca^{2+}-free saline solution, converted the firing pattern to a bursting mode. Adding 25 μM NH6 (*A*) or 10 μM retigabine (*B*) to the Ca^{2+}-free saline solution suppressed the burst response by decreasing the underlying spike ADP.

6, $P < 0.01$), higher drug concentration ($\geq$10 μM) totally suppressed the occurrence of spontaneous EPSCs (Fig. 6, *B, C,* and *E*). Noteworthy, the inhibitory effect of NH6 on EPSC frequency was completely reversible (Fig. 6, *B* and *C*). In contrast, addition of the M-channel blocker linopirdine (25 μM) increased the frequency of spontaneous EPSCs by 278 $\pm$ 41% of control ($n = 5$, $P < 0.01$), reflecting the existence of a substantial tonic M-channel activity (Fig. 6*D*). These results

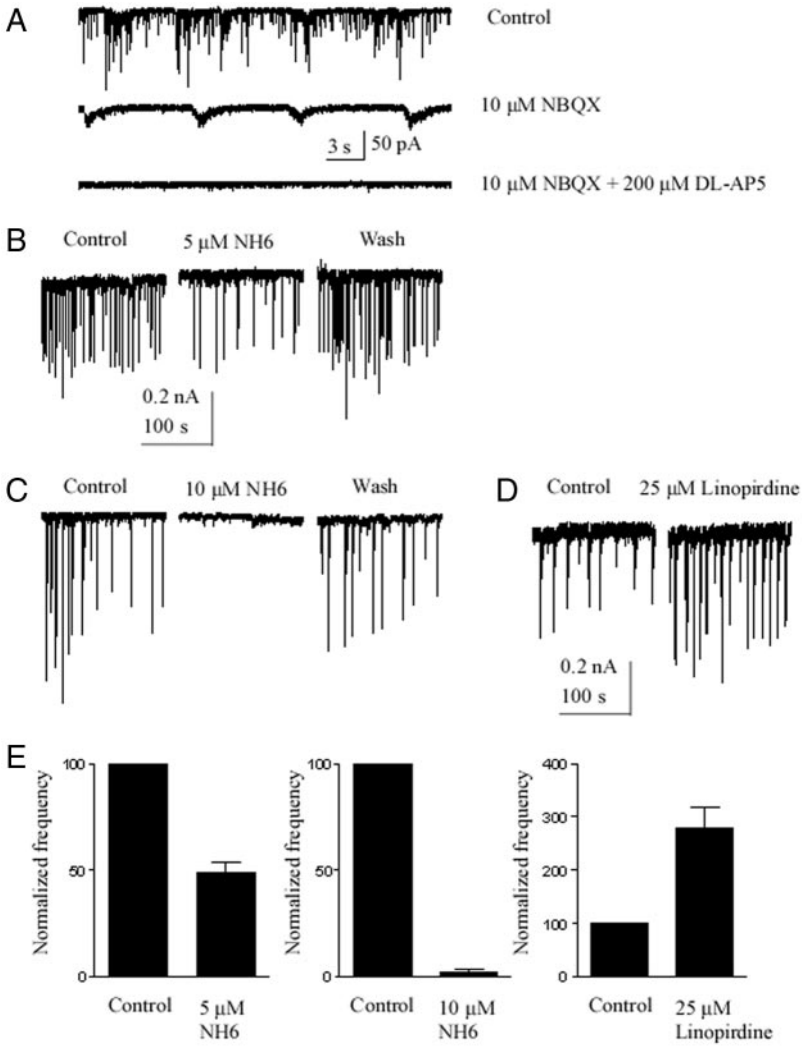

FIG. 6. NH6 reduces the frequency of spontaneous excitatory postsynaptic currents (EPSCs) in cultured hippocampal neurons. *A*: representative traces of spontaneous EPSCs recorded at a holding potential of -70 mV. The main component of spontaneous EPSCs is mediated by AMPA receptors as they were mostly blocked by 10 μM 1,2,3,4-tetrahydro-6-nitro-2,3-dioxo-benzo[f]quinoxaline-7-sulfonamide (NBQX). A minor fraction of EPSPs resistant to NBQX was abolished by D-2-amino-5-phosphonopentanoic acid, suggesting that they are also mediated by *N*-methyl-D-aspartate (NMDA) receptors, though to a much lower extent. *B* and *C*: EPSC bursting frequency was reversibly depressed by 5 μM NH6 (*B*) and totally suppressed by 10 μM NH6 (*C*). *D*: EPSC bursting frequency was increased in the presence of 25 μM linopirdine. *E*: summary data of the impact of 5 μM NH6 (*left*), 10 μM NH6 (*middle*), and 25 μM linopirdine (*right*) on the normalized number of bursts recorded in 180-s time period ($n = 5$–6).

are summarized in Fig. 6*E*. They are consistent with the findings showing that NH6 suppresses the spontaneous discharge of hippocampal neurons (Fig. 4) but do not distinguish between its effects on intrinsic excitability and on synaptic transmission. Interestingly, application of NH6 also reduced the frequency of spontaneous inhibitory IPSCs recorded from cultured hippocampal neurons (manuscript in preparation).

Activation of M-channels by NH6 does not affect the amplitude and the kinetics of miniature EPSCs and IPSCs but decreases their frequency

To examine further a possible synaptic site of NH6 action, we analyzed its effects on mEPSCs and mIPSCs, which reflect the spontaneous release of transmitter quanta independent of spike discharge. To that end, the cultured hippocampal neurons were bathed in solutions containing 0.5 μM TTX. We recorded mEPSPs and mIPSPs separately by blocking, respectively, $GABA_A$ (with 10 μM picrotoxin and 10 μM bicuculline) or AMPA receptors (with 10 μM NBQX). In all experiments, the holding membrane potential was -70 mV.

The effects of NH6 on mEPSPs are illustrated in Fig. 7. Adding 10 μM NH6 to the external solution consistently reduced mEPSP frequency (Fig. 7*A*). In six such experiments NH6 decreased mEPSP frequency by ~50% (from 0.21 ± 0.06 to 0.10 ± 0.02 Hz; $P < 0.01$). This effect is illustrated in Fig. 7*E* which shows the cumulative frequency distribution of mEPSCs before (control) and during exposure to 10 μM NH6. Clearly, NH6 significantly shifts this distribution to longer interevent intervals (Fig. 7*E*).

In principle, the observed reduction in mEPSP frequency by NH6 may be due to presynaptic inhibition of glutamate release or to postsynaptic block of AMPA receptors or both. To distinguish between these possibilities, we monitored the amplitudes and kinetics of the mEPSPs, which should be unaffected if NH6 acts exclusively presynaptically. Figure 7*C* illustrates the typical time course of a mEPSC before (control) and during exposure to 10 μM NH6. Under control recording conditions, the mEPSC amplitude, 10–90% rise time, and decay time constant were, respectively, -24.1 ± 3.5 pA, 0.7 ± 0.1 ms, and 11.2 ± 2.0 ms ($n = 5$). In the presence of NH6, the values of the amplitude, the rise time and decay kinetics of mEPSCs corresponded to -22.9 ± 1.4 pA, 0.8 ± 0.1 ms, and 13.2 ± 2.0 ms, respectively ($n = 5$; Fig. 7*B*). In summary, NH6 affected neither the amplitude of mEPSCs nor their kinetics of rise and decay (Fig. 7, *B–D*), suggesting that the novel M-channel opener does not interact with postsynaptic AMPA receptors. Thus these data suggest that M-channel activation by NH6 could presynaptically inhibit the spontaneous quantal release of glutamate. To further investigate this possibility, we explored the effects of the M-channel blocker linopirdine on mEPSCs (Fig. 8). In six of nine pyramidal neurons examined, 20 μM linopirdine added to the extracellular solution, significantly increased mEPSP frequency (Fig. 8*A,C*). Linopirdine reversibly enhanced mEPSP frequency by about fivefold (from 0.31 ± 0.07 to 1.56 ± 0.12 Hz; $n = 6$; $P < 0.01$). This effect is illustrated in Fig. 8*C* which shows the cumulative frequency distribution of mEPSCs before (control), after exposure to 20 μM linopirdine and after washout of the drug (wash). Clearly, linopirdine significantly shifts this distribution to shorter interevent intervals (Fig. 8*C*). In contrast, linopirdine did not affect the amplitude of mEPSCs which was -25.3 ± 1.7 and -24.1 ± 1.2 pA in the absence and presence of the blocker, respectively ($n = 9$). This is illustrated in Fig. 8*B,* which shows the cumulative amplitude distribution of mEPSCs before (control), after exposure to 20 μM linopirdine. In addition, when 10 μM NH6 was co-applied with 20 μM linopirdine no change in mEPSP frequency was observed (not shown).

Similar results were obtained in experiments testing the effects of NH6 on mIPSCs, as illustrated in Fig. 9. Thus 10 μM NH6 significantly reduced mIPSC frequency by ~58% (from 0.42 ± 0.21 to 0.18 ± 0.07 Hz; $P < 0.01$; $n = 6$). This feature is illustrated in Fig. 9*E*, which shows the cumulative frequency distribution of mIPSCs before (control) and during exposure to 10 μM NH6. Like for mEPSCs, NH6 notably shifted the

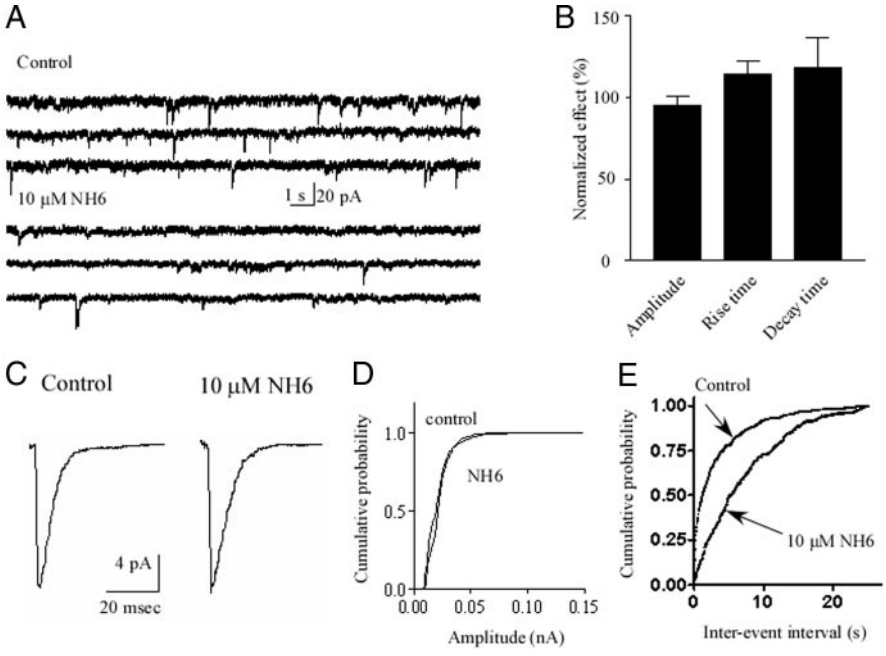

FIG. 7. M-channel activation by NH6 reduces the frequency of miniature EPSCs (mEPSCs) in cultured hippocampal neurons. *A*: representative records of mEPSCs recorded before (*top*) and after (*bottom*) application of 10 μM NH6. *B*: effect of NH6 on normalized on amplitude, rise time and decay time constants ($n = 5$). *C*: representative single mEPSC waveform before (control) and after 10 μM NH6. *D*: cumulative probability plots for current amplitude showing that NH6 did not affect the mEPSC amplitude ($n = 5$). *E*: cumulative probability plots for mEPSC interevent intervals before (control), after exposure of 10 μM NH6 showing that NH6 reduces the frequency of mEPSCs ($n = 6$).

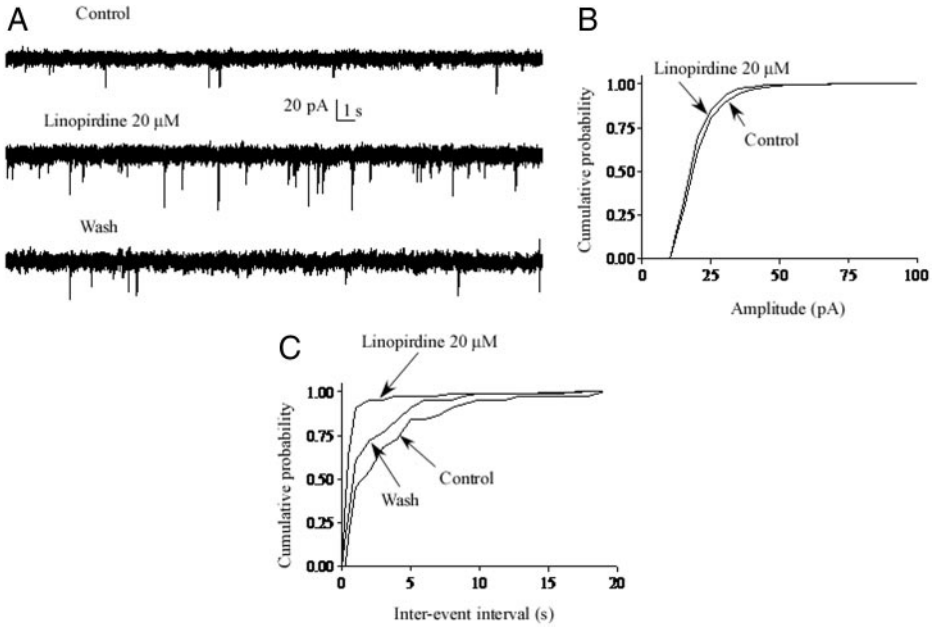

FIG. 8. M-channel blockade by linopirdine increases the frequency of mEPSCs in cultured hippocampal neurons. *A*: representative records of mEPSCs recorded before (*top*), after application of 20 μM linopirdine (*middle*), and after wash (*bottom*). *B*: cumulative probability plots for current amplitude showing that 20 μM linopirdine did not affect the mEPSC amplitude ($n = 9$). *C*: cumulative probability plots for mEPSC interevent intervals before (control), after exposure of 20 μM linopirdine, and after wash. Linopirdine significantly shifts the distribution of interevent intervals to the left, indicating that it significantly increased the mEPSCs frequency ($n = 6$).

mIPSC frequency distribution to longer interevent intervals (Fig. 9*E*). Neither the amplitude nor the rise and decay kinetics of mIPSCs were significantly altered by NH6 (Fig. 9, *A–D*). Under control recording conditions, the mIPSC amplitude, 10–90% rise time, and decay time constant were, respectively, 32.0 ± 3.2 pA, 0.8 ± 0.1 ms, and 26.1 ± 3.1 ms ($n = 6$). In the presence of NH6, the values of the amplitude, the rise time, and decay kinetics of mIPSCs represented 29.8 ± 1.3 pA, 0.9 ± 0.1 ms, and 29.0 ± 2.0 ms, respectively ($n = 6$; Fig. 9*B*). This lack of action on mIPSC amplitude and waveform suggests that NH6 does not affect the properties of postsynaptic $GABA_A$ receptors. Thus the results suggest that M-channel activation by NH6 could also inhibit the presynaptic quantal release of GABA.

DISCUSSION

In this work, we investigated the presence and functions of pre- and postsynaptic M-channels using a novel Kv7.2/3 channel opener, NH6, which we synthesized as a new derivative of *N*-phenylanthranilic acid. Our results indicate that M-channels act both pre- and postsynaptically to modulate neuronal excitability. On the one hand, the depressant action of NH6 on spike discharge and spike ADPs reflects the presence of postsynaptic M-channels, likely located at the soma/axon hillock region of the neuron (Chung et al. 2006; Devaux et al. 2004). On the other hand, the depression of mEPSCs and mIPSPs frequencies by NH6 indicates that M-channels are also present at or near presynaptic terminals. The good selectivity of NH6 for M-channels versus other Kv channels and NMDA, AMPA and

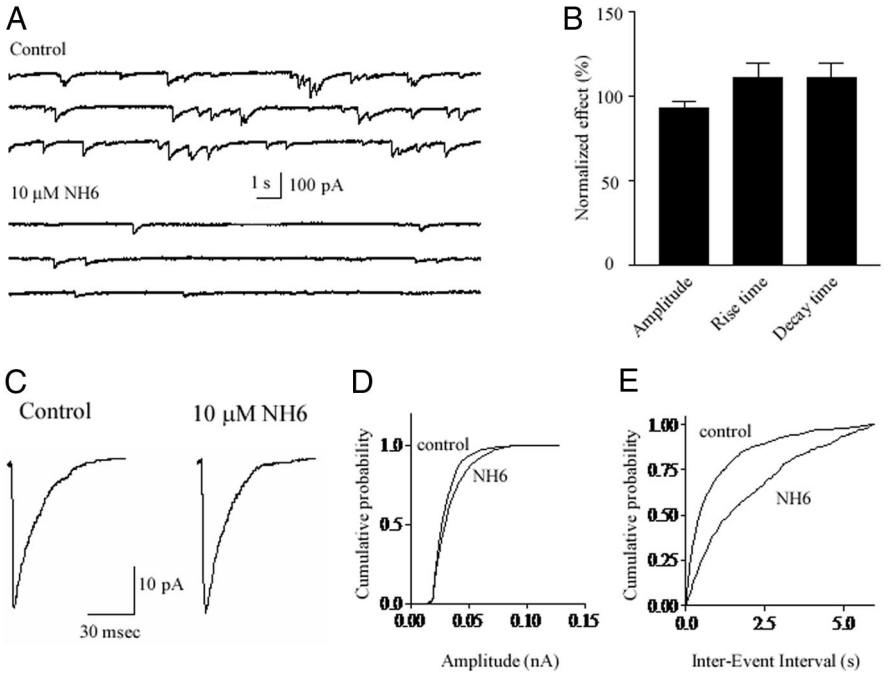

FIG. 9. M-channel activation by NH6 reduces the frequency of mIPSCs in cultured hippocampal neurons. *A*: representative traces of miniature inhibitory postsynaptic currents (mIPSCs) recorded before (*top*) and after (*bottom*) application of 10 μM NH6. *B*: effect of NH6 on normalized on amplitude, rise time, and decay time constants ($n = 6$). *C*: representative single mIPSC waveform before (control) and after 10 μM NH6. *D*: cumulative probability plots for current amplitude showing that NH6 did not significantly affect the mIPSC amplitude ($n = 6$). *E*: cumulative probability plots for mIPSC interevent intervals before (control) and after exposure of 10 μM NH6, showing that NH6 depresses the frequency of mIPSCs ($n = 6$).

$GABA_A$ receptors provides a new pharmacological tool for exploring the biophysical and pathophysiological properties of M-currents.

Targeting M-channels is of clinical importance and several drugs that modulate both recombinant Kv7.2/3 channels and native M-currents have been characterized (Brown and Yu 2000; Robbins 2001). For example, the anticonvulsant drug retigabine, and more recently acrylamide derivatives, were characterized as Kv7.2/3 channel openers (Blackburn-Munro and Jensen 2003; Passmore et al. 2003; Tatulian et al. 2001; Wu et al. 2004). In this study, we have synthesized and characterized the neurophysiological properties of a novel compound NH6, using diclofenac as a primary template which defines a new class of Kv7.2/3 channel openers. Indeed, we recently showed that diclofenac, a derivative of *N*-phenylanthranilic acid, activates recombinant Kv7.2/3 channels and native M-current (Peretz et al. 2005). NH6 shifts the voltage dependence of Kv7.2/3 channel activation toward more negative potentials, slows down deactivation kinetics, and hyperpolarizes the resting membrane potential in most neurons. The extent to which NH6 enhances the Kv7.2/3 currents is voltage dependent. Although large increases in Kv7.2/3 currents are seen at threshold potentials (−60 to −40 mV), weaker opener responses are seen at depolarized potential values above −30 mV. These voltage-dependent effects of NH6 are similar to those displayed by structurally unrelated openers like retigabine and acrylamide derivatives (Tatulian et al. 2001; Wu et al. 2004). The voltage-dependent action of retigabine was suggested to arise from a secondary inhibitory effect of the drug at more depolarized potentials (Tatulian and Brown 2003; Tatulian et al. 2001). Although this possibility is likely for NH6, there are additional plausible mechanisms. For example, if NH6 acts by increasing the channel open probability (Po), its impact may be maximal at threshold potentials where the voltage-dependent Kv7.2/3 channels exhibit a low Po in the absence of the drug. However, at depolarized potentials the channel Po may reach saturating values that could not be further boosted by the opener. Alternatively, the NH6 binding site may reside deep in the membrane electric field in such a way that the drug association or dissociation rates will, respectively, decrease or increase at depolarized potentials. There are interesting differences between retigabine and NH6 with respect to their selectivity toward other ion channels. Retigabine potently reduces the excitability of neural circuits not only by opening M-channels but also by augmenting GABAergic IPSCs via a postsynaptic interaction with $GABA_A$ receptors (Otto et al. 2002). In contrast, NH6 changed neither the amplitude of bicuculline-sensitive mIPSCs currents nor their kinetics of rise and decay, suggesting that it does not affect the properties of postsynaptic $GABA_A$ receptors. Along this line, NH6 was ineffective toward recombinant NR1/NR2B and NMDA and AMPA receptor-mediated EPSCs. Likewise, NH6 did not affect the amplitude of currents carried by several types of voltage-activated K^+ channels. Recent studies suggested that retigabine binds to a hydrophobic pocket formed on channel opening between the cytoplasmic parts of S5 and S6 (Schenzer et al. 2005; Wuttke et al. 2005). It is not clear yet whether NH6 binds to the same channel site; however, we recently showed that the opener effects of retigabine and meclofenamic acid, a derivative of NH6, are additive rather than mutually occlusive, suggesting that retigabine and NH6 may act on independent sites of Kv7.2/3 channels (Peretz et al. 2005).

Using different neuronal systems, including DRG, cortical, and hippocampal cultured neurons as well as CA1 pyramidal cells in hippocampal slices, we showed that enhancement of M-currents by NH6 profoundly depresses both evoked and spontaneous neuronal firing. This effect is readily explained by the opener action of NH6 on M-channels. By shifting the M-current activation curve negatively and by slowing the deactivation kinetics, NH6 induces substantial M-channel activation at resting and subthreshold potentials. Our finding that NH6 suppresses spiking activity in DRG neurons is in line with recent data showing that Kv7./M-channels are also present in nociceptive sensory cells (Passmore et al. 2003).

Although Kv7.2 and Kv7.3 immunoreactive proteins are expressed on somata and dendrites of hippocampal and neocortical pyramidal and polymorphic neurons (Cooper et al. 2000, 2001), recent studies found that these proteins cluster at nodes of Ranvier and axon initial segments (Chung et al. 2006; Devaux et al. 2004; Pan et al. 2006). Many axon initial segments of pyramidal neurons in hippocampal CA1 and CA3 layers and of temporal neocortex express both Kv7.2 and Kv7.3 subunits. The axon initial segment is a strategic site for M-channels to shape the spike ADP waveform and modulate spike-frequency adaptation (Gu et al. 2005; Yue and Yaari 2004, 2006). Thus Kv7.2/3 channel activity may influence intrinsic excitability at the initial segment, where fast spikes (Colbert and Johnston 1996) and probably also spike ADPs (Yue et al. 2005) are initiated. The action of Kv7.2/3 at this site may be modulated by neurotransmitters released at axo-axonic synapses. In line with previous data (Yue and Yaari 2004), we found that activation of M-channels by NH6 and retigabine robustly depresses the spike ADP and associated bursting in CA1 pyramidal cells. In adult CA1 pyramidal neurons, spike ADPs are driven primarily by the persistent Na^+ current (I_{NaP}), which activates at subthreshold potentials (Azouz et al. 1996; Su et al. 2001). Thus the size of the spike ADP would depend on the interplay between I_{NaP}, which would tend to enhance the ADP to the point of bursting, and I_M, which would curtail the ADP and prevent repetitive discharge (Yue and Yaari 2004, 2006). The production of high-frequency spike bursting may play a major role in triggering epileptiform discharges when GABA-mediated synaptic inhibition is compromised (Yaari and Beck 2002). Therefore we expect that NH6 and its derivatives will manifest anticonvulsant activity. Interestingly, we recently prepared an amide derivative of NH6 which displays anticonvulsant activity in mice with an ED_{50} of 8.7 mg/kg, when measured by the maximal electroshock test (Peretz and Attali, unpublished data).

The present results showing that NH6 reduces mEPSC and mIPSC frequencies without altering their amplitude or kinetics suggest a role for presynaptic M-channels in regulating neurotransmitter release. Our data are in line with a recent work showing that M-channel activation inhibits the release of loaded [^{3}H] norepineprine, [^{3}H] GABA, and [^{3}H] D-aspartate from hippocampal synaptosomes (Martire et al. 2004). In the hippocampus, Kv7.2 but not Kv7.3 immunoreactivity is expressed presynaptically on axons and nerve terminals of the mossy fiber pathway in both mouse and human brain (Cooper et al. 2000, 2001). Noteworthy, a recent study showed that Kv7.2 and Kv7.3 immunoreactive proteins are not only ex-

pressed in axon initial segments but also in distal axons and presynaptic terminals of cultured hippocampal neurons (Chung et al. 2006). Hence, Kv7.2/3 expression in distal axons and presynaptic terminals may allow the dynamic tuning by M-channels of action potential propagation along the axon and neurotransmitter release from the nerve terminal. M-channels are also expressed in nociceptive afferent terminals of DRG neurons where their activation would also lead to a decrease in peripheral neurotransmitter release (Passmore et al. 2003). Although we cannot totally exclude that NH6 could act via additional mechanisms unrelated to Kv7.2/3, a plausible explanation for this presynaptic inhibitory action is that M-channel activation hyperpolarizes the presynaptic terminals, thereby directly or indirectly depressing spontaneous vesicular transmitter release. Along this line, the linopirdine-induced increase in mEPSC frequency further strengthens this proposal. It is possible, however, that a more complex interaction exists between M-channels and the presynaptic release machinery downstream of Ca^{2+} entry (Linial et al. 1997; Parnas et al. 2000). Surprisingly, a recently published work indicates that activation of presynaptic M-channels by retigabine at glutamatergic pathways in the CA1 hippocampal area, enhances the axonal action potential and transmitter release under elevated external potassium concentrations (Vervaeke et al. 2006). Although a presynaptic potassium current is normally expected to reduce excitability and release, the authors interpret their rather unexpected result by suggesting that opening of M-channels in axons terminals will boost the spike-dependent transmitter release by reducing Na^+ channel inactivation (Vervaeke et al. 2006). We have no explanations yet for this seemingly opposite result compared with the present study and to that of Martire et al. (2004), who found that activation of M-channels by retigabine inhibits transmitter release in hippocampal synaptosomes (Martire et al. 2004). It is possible that glutamatergic terminals respond differently to M-channel activation under high external K^+ in slices compared with synaptically active terminal network in cultured neurons. In this regard, NH6 will be an excellent pharmacological tool to investigate the presynaptic impact of M-channel activation because unlike retigabine (Otto et al. 2002), it does not affect postsynaptic $GABA_A$ receptor currents.

The presynaptic inhibition of transmitter release can be effected by various mechanisms which include activation of presynaptic G-protein-coupled receptors, such as the $GABA_B$, adenosine, or cannabinoid receptors that act by inhibiting voltage-gated Ca^{2+} channels or by operating downstream of Ca^{2+} entry (Wu and Saggau 1997). Presynaptic $GABA_A$ receptors can also depress transmitter release by a shunting mechanism or by inactivating voltage-gated Na^+ and/or Ca^{2+} channels (Kullmann et al. 2005; Stuart and Redman 1992). Activation of presynaptic M-channels provides an additional mechanism of presynaptic inhibition that might serve as a mean of adjusting synaptic strength and preventing excessive transmitter release. M-channels in hippocampal neurons are modulated by multiple neurotransmitters (reviewed by Marrion 1997). Reflecting the existence of a tonic modulation of M-current activity, we found that the addition of the M-channel blocker linopirdine robustly increases the frequency of spontaneous EPSCs by ~2.8-fold. The presynaptic inhibition of glutamate and GABA release, acting in concert with the postsynaptic depression of somatic spike ADP and associated bursting, would reduce excitability of pyramidal neurons and limit the spread of burst discharges through the hippocampus. These actions of M-channels may be particularly important in preventing seizures in the early postnatal period, during which GABAergic neurotransmission excites, rather than inhibits, the pyramidal neurons (reviewed by (Ben-Ari 2002; Yaari and Beck 2002).

GRANTS

This work is supported by the Israel Science Foundation (ISF 672/05), by US-Israel Binational Science Foundation Grant 2001229, and the Keren Wolfson funds to B. Attali.

We thank Dr. Thomas Jentsch for providing the Kv7.2 and Kv7.3 cDNA clones.

REFERENCES

Aiken SP, Brown WM. Treatment of epilepsy: existing therapies and future developments. *Front Biosci* 5: E124–E152, 2000.

Azouz R, Jensen MS, Yaari Y. Ionic basis of spike after-depolarization and burst generation in adult rat hippocampal CA1 pyramidal cells. *J Physiol* 492: 211–223, 1996.

Ben-Ari Y. Excitatory actions of gaba during development: the nature of the nurture. *Nat Rev Neurosci* 3: 728–739, 2002.

Biervert C, Schroeder BC, Kubisch C, Berkovic SF, Propping P, Jentsch TJ, Steinlein OK. A potassium channel mutation in neonatal human epilepsy. *Science* 279: 403–406, 1998.

Birch PJ, Dekker LV, James IF, Southan A, Cronk D. Strategies to identify ion channel modulators: current and novel approaches to target neuropathic pain. *Drug Discovery Today* 9: 410–418, 2004.

Blackburn-Munro G, Jensen BS. The anticonvulsant retigabine attenuates nociceptive behaviours in rat models of persistent and neuropathic pain. *Eur J Pharmacol* 460: 109–116, 2003.

Brown BS, Yu SP. Modulation and genetic identification of the M channel. *Prog Biophys Mol Biol* 73: 135–166, 2000.

Brown DA. M-currents. In: *In Ion channels.* New York: Plenum, 1988, p. 55–99.

Brown DA, Adams PR. Muscarinic suppression of a novel voltage-sensitive K^+ current in a vertebrate neurone. *Nature* 283: 673–676, 1980.

Chung HJ, Jan YN, Jan LY. Polarized axonal surface expression of neuronal KCNQ channels is mediated by multiple signals in the KCNQ2 and KCNQ3 C-terminal domains. *Proc Natl Acad Sci USA* 103: 8870–8875, 2006.

Colbert CM, Johnston D. Axonal action-potential initiation and Na^+ channel densities in the soma and axon initial segment of subicular pyramidal neurons. *J Neurosci* 16: 6676–6686, 1996.

Cooper EC, Aldape KD, Abosch A, Barbaro NM, Berger MS, Peacock WS, Jan YN, Jan LY. Colocalization and coassembly of two human brain M-type potassium channel subunits that are mutated in epilepsy. *Proc Natl Acad Sci USA* 97: 4914–4919, 2000.

Cooper EC, Harrington E, Jan YN, Jan LY. M channel KCNQ2 subunits are localized to key sites for control of neuronal network oscillations and synchronization in mouse brain. *J Neurosc* 21: 9529–9540, 2001.

Cooper EC, Jan LY. M-channels: neurological diseases, neuromodulation, and drug development. *Arch Neurol* 60: 496–500, 2003.

Dedek K, Kunath B, Kananura C, Reuner U, Jentsch TJ, Steinlein OK. Myokymia and neonatal epilepsy caused by a mutation in the voltage sensor of the KCNQ2 K^+ channel. *Proc Natl Acad Sci USA* 98: 12272–12277, 2001.

Devaux JJ, Kleopa KA, Cooper EC, Scherer SS. KCNQ2 is a nodal K^+ channel. *J Neurosci* 24: 1236–1244, 2004.

Geiger J, Weber YG, Landwehrmeyer B, Sommer C, Lerche C. Immunohistochemical analysis of KCNQ3 potassium channels in mouse brain. *Neurosci Lett* 400: 101–104, 2006.

Gu N, Vervaeke K, Hu H, Storm JF. Kv7/KCNQ/M and HCN/h, but not KCa2/SK channels, contribute to the somatic medium after-hyperpolarization and excitability control in CA1 hippocampal pyramidal cells. *J Physiol* 566: 689–715, 2005.

Hamill OP, Marty A, Neher E, Sakmann B, Sigworth FJ. Improved patch-clamp techniques for high resolution current recording from cells and cell-free membrane patches. *Pfluegers* 391: 85–100, 1981.

Jentsch TJ. Neuronal KCNQ potassium channels:physiology and role in diseases. *Nat Neurosci* 1: 21–30, 2000.

Jurman ME, Boland LM, Liu Y, Yellen G. Visual identification of individual transfected cells for electrophysiology using antibody-coated beads. *Biotechniques* 17: 876–881, 1994.

Kullmann DM, Ruiz A, Rusakov DM, Scott R, Semyanov A, Walker MC. Presynaptic, extrasynaptic and axonal GABAA receptors in the CNS: where and why? *Prog Biophys Mol Biol* 87: 33–46, 2005.

Lerche C, Scherer CR, Seebohm G, Derst C, Wei AD, Busch AE, Steinmeyer K. Molecular cloning and functional expression of KCNQ5, a potassium channel subunit that may contribute to neuronal M-current diversity. *J Biol Chem* 275: 22395–22400, 2000.

Linial M, Ilouz N, Parnas H. Voltage-dependent interaction between the muscarinic ACh receptor and proteins of the exocytic machinery. *J Physiol* 504: 251–258, 1997.

Marrion NV. Control of M-current. *Annu Rev Physiol* 59: 483–504, 1997.

Martire M, Castaldo P, D'Amico M, Preziosi P, Annunziato L, Taglialatela M. M channels containing KCNQ2 subunits modulate norepinephrine, aspartate, and GABA release from hippocampal nerve terminals. *J Neurosci* 24: 592–597, 2004.

Otto JF, Kimball MM, Wilcox KS. Effects of the anticonvulsant Retigabine on cultured cortical neurons: changes in electroresponsive properties and synaptic transmission. *Mol Pharmacol* 61: 921–927, 2002.

Pan Z, Kao T, Horvath Z, Lemos J, Sul J-Y, Cranstoun SD, Bennett V, Scherer SS, Cooper EC. A common ankyrin-G-based mechanism retains KCNQ and Na_V channels at electrically active domains of the axon. *J Neurosci* 26: 2599–2613, 2006.

Parnas H, Segel L, Dudel J, Parnas I. Autoreceptors, membrane potential and the regulation of transmitter release. *Trends Neurosci* 23: 60–68, 2000.

Passmore GM, Selyanko AA, Mistry M, Al-Qatari M, Marsh SJ, Matthews EA, Dickenson AH, Brown TA, Burbidge SA, Main M, Brown DA. KCNQ/M currents in sensory neurons: significance for pain therapy. *J Neurosci* 23: 7227–7236, 2003.

Peretz A, Degani N, Nachman R, Uziyel Y, Gibor G, Shabat D, Attali B. Meclofenamic acid and diclofenac, novel templates of KCNQ2/Q3 potassium channel openers, depress cortical neuron activity and exhibit anticonvulsant properties. *Mol Pharmacol* 67: 1053–1066, 2005.

Peters HC, Hu H, Pongs O, Storm JF, Isbrandt D. Conditional transgenic suppression of M channels in mouse brain reveals functions in neuronal excitability, resonance and behavior. *Nat Neurosci* 8: 51–60, 2005.

Robbins J. KCNQ potassium channels: physiology, pathophysiology, and pharmacology. *Pharmacol Ther* 90: 1–19, 2001.

Rogawski MA. KCNQ2/KCNQ3 K^+ channels and the molecular pathogenesis of epilepsy: implications for therapy. *Trends Neurosci* 23: 393–398, 2000.

Rundfeldt C, Netzer R. Investigations into the mechanism of action of the new anticonvulsant retigabine. Interaction with GABAergic and glutamatergic neurotransmission and with voltage gated ion channels. *Arzneimittelforschung* 50: 1063–1070, 2000.

Schenzer A, Friedrich T, Pusch M, Saftig P, Jentsch TJ, Grotzinger J, Schwake M. Molecular determinants of KCNQ (Kv7) K^+ channel sensitivity to the anticonvulsant retigabine. *J Neurosci* 25: 5051–5060, 2005.

Schnee ME, Brown BS. Selectivity of linopirdine (DuP 996), a neurotransmitter release enhancer, in blocking voltage-dependent and calcium-activated potassium currents in hippocampal neurons. *J Pharmacol Exp Therap* 286: 709–717, 1998.

Schroeder BC, Hechenberger M, Weinreich F, Kubisch C, Jentsch TJ. KCNQ5, a novel potassium channel broadly expressed in brain, mediates M-type currents. *J Biol Chem* 275: 24089–24095, 2000.

Shah MM, Mistry M, Marsh SJ, Brown DA, Delmas P. Molecular correlates of the M-current in cultured rat hippocampal neurons. *J Physiol* 544: 29–37, 2002.

Singh NA, Charlier C, Stauffer D, DuPont BR, Leach RJ, Melis R, Ronen GM, Bjerre I, Quattlebaum T, Murphy JV, McHarg ML, Gagnon D, Rosales TO, Peiffe A, Anderson VE, Leppert M. A novel potassium channel gene, KCNQ2, is mutated in an inherited epilepsy of newborns. *Nat Genet* 8: 25–29, 1998.

Storm JF. Potassium currents in hippocampal pyramidal cells. *Prog Brain Res* 83: 161–187, 1990.

Stuart GJ, Redman SJ. The role of GABAA and GABAB receptors in presynaptic inhibition of Ia EPSPs in cat spinal motoneurones. *J Physiol* 447: 675–692, 1992.

Su H, Alroy G, Kirson ED, Yaari Y. Extracellular calcium modulates persistent sodium current-dependent burst-firing in hippocampal pyramidal neurons. *J Neurosci* 21: 4173–4182, 2001.

Tatulian L, Brown DA. Effect of the KCNQ potassium channel opener retigabine on single KCNQ2/3 channels expressed in CHO cells. *J Physiol* 549: 57–63, 2003.

Tatulian L, Delmas P, Abogadie FC, Brown DA. Activation of expressed KCNQ potassium currents and native neuronal M-type potassium currents by the anti-convulsant drug retigabine. *J Neurosci* 21: 5535–5545, 2001.

Vervaeke K, Gu N, Agdestein C, Hu H, Storm J. Kv7/KCNQ/M-channels in rat glutamatergic hippocampal axons and their role in regulation of excitability and transmitter release. *J Physiol* 576: 235–256, 2006.

Wang H-S, Pan Z, Shi W, Brown BS, Wymore RS, Cohen IS, Dixon JE, McKinnon D. KCNQ2 and KCNQ3 potassium channel subunits: molecular correlates of the M-channel. *Science* 282: 1890–1893, 1998.

Weber YG, Geiger J, Kampchen K, Landwehrmeyer B, Sommer C, Lerche C. Immunohistochemical analysis of KCNQ2 potassium channels in adult and developing mouse brain. *Brain Res* 1077: 1–6, 2006.

Wickenden AD, Yu W, Zou A, Jegla T, Wagoner PK. Retigabine, a novel anti-convulsant, enhances activation of KCNQ2/Q3 potassium channels. *Mol Pharmacol* 58: 591–600, 2000.

Wu LG, Saggau P. Presynaptic inhibition of elicited neurotransmitter release. *Trends Neurosci* 20: 204–212, 1997.

Wu YJ, He H, Sun LQ, L'Heureux A, Chen J, Dextraze P, Starrett JE, Jr, Boissard CG, Gribkoff VK, Natale J, Dworetzky SI. Synthesis and structure-activity relationship of acrylamides as KCNQ2 potassium channel openers. *J Med Chem* 47: 2887–2896, 2004.

Wuttke TV, Seebohm G, Bail S, Maljevic S, Lerche H. The new anticonvulsant retigabine favors voltage-dependent opening of the Kv7.2 (KCNQ2) channel by binding to its activation gate. *Mol Pharmacol* 67: 1009–1017, 2005.

Yaari Y, Beck H. "Epileptic neurons" in temporal lobe epilepsy. *Brain Pathol* 12: 234–239, 2002.

Yue C, Remy S, Su H, Beck H, Yaari Y. Proximal persistent Na^+ channels drive spike afterdepolarizations and associated bursting in adult CA1 pyramidal cells. *J Neurosci* 25: 9704–9720, 2005.

Yue C, Yaari Y. KCNQ/M channels control spike afterdepolarization and burst generation in hippocampal neurons. *J Neurosci* 24: 4614–4624, 2004.

Yue C, Yaari Y. Axo-somatic and apical dendritic Kv7/M channels differentially regulate the intrinsic excitability of adult rat CA1 pyramidal cells. *J Neurophysiol* 95: 3480–3495, 2006.